Nonlinear Dynamical Characterization of Heart Rate Variability Time Series of Meditation

B. S. Raghavendra, and D. Narayana Dutt

Abstract—Many recent electrophysiological studies have revealed the importance of investigating meditation state in order to achieve an increased understanding of autonomous control of cardiovascular functions. In this paper, we characterize heart rate variability (HRV) time series acquired during meditation using nonlinear dynamical parameters. We have computed minimum embedding dimension (MED), correlation dimension (CD), largest Lyapunov exponent (LLE), and nonlinearity scores (NLS) from HRV time series of eight Chi and four Kundalini meditation practitioners. The pre-meditation state has been used as a baseline (control) state to compare the estimated parameters. The chaotic nature of HRV during both pre-meditation and meditation is confirmed by MED. The meditation state showed a significant decrease in the value of CD and increase in the value of LLE of HRV, in comparison with pre-meditation state, indicating a less complex and less predictable nature of HRV. In addition, it was shown that the HRV of meditation state is having highest NLS than pre-meditation state. The study indicated highly nonlinear dynamic nature of cardiac states as revealed by HRV during meditation state, rather considering it as a quiescent state.

Keywords—Correlation dimension, Embedding dimension, Heart rate variability, Largest Lyapunov exponent, Meditation, Nonlinearity score.

I. INTRODUCTION

MEDITATION is an ancient spiritual practice with a potential benefit on health and well-being [1], [2]. It is a holistic system of mind-body practice for mental and physical health. This practice incorporates multiple techniques including breathing exercise, sustained concentration, physical posture, and many more. Indeed, meditation is considered as an altered state of consciousness different from ordinary wake and sleep states. Recently, the electrophysiological studies have revealed the importance of investigating the state changes related to meditation in order to achieve increased understanding of physiology in general. In this direction, many studies have focused on the physiological effect of different meditation techniques to gain insight into the physiological prerequisites responsible for the improvement of health [3]-[10].

Various studies carried out with meditation practitioners have suggested a number of physiological changes. It is said that during meditation, the body is under a hypometabolic state and controlled most of the time by parasympathetic nervous system [11], reduction or variability in heart rate [7], modifications in the concentrations of neurotransmitters [12], a drop in oxygen uptake as well as in carbon dioxide output [13], [11]. The use of meditation practice is becoming more popular to reduce stress, and effective as a complementary treatment for many disorders, such as hypertension, anxiety and insomnia [14], [15]. The meditation is associated with physiological signs of altered activation of autonomic and endocrine systems. This is evident from the studies of increased level of skin resistance and reduced levels of heart rate, blood-lactate level, cortisol, and respiration rate [16], [17], [12], [18].

The meditation practice has improved the self-rated quality of sleep in older persons compared to a group receiving an ayurveda poly-herbal preparation and another wait-list control group [19]. Meditation practice has shown to reduce stress and increase feelings of calm [20]. In normal volunteers, meditation has shown reduced psychophysiological arousal based on a decrease in oxygen consumption [21], [22], and changes in heart rate variability suggestive of a shift towards vagal dominance [23], decreased occupational stress levels and baseline autonomic arousal [24]. Studies have shown that meditation practice can improve mood [25], [26], increase resilience to chronic and acute stress [27], [28], enhanced performance on a variety of cognitive [29], [30], psychomotor [31], [30], and physical [25], [32] tasks.

Meditation is a complex physiological process which affects neural, psychological, behavioral, and autonomic functions, and is considered as an altered state of consciousness, differing from wakefulness, relaxation at rest, and sleep [33]-[35]. There are many evidences to the fact that meditation practice leads to functional changes in physiological states of humans [36]-[38], [12]. Most of the meditation techniques work by affecting the ANS, in turn regulating many organs and muscles, controlling functions such as the heart beat, sweating, breathing, and digestion. One possible way for meditation to act on autonomic activity is through respiration control. Respiration is one of the few body autonomic functions that can be controlled and can affect functioning of the ANS [39], [40]. Many meditation traditions consider breath, body and mind as linked, and thus have given the breath a central role in meditation practice. Slower respiration rate during meditation practice induces changes in the cardiovascular activity that corresponds to an increase in

B. S. Raghavendra and D. Narayana Dutt are with the Department of Electrical Communication Engineering, Indian Institute of Science, Bangalore – 560 012, India (corresponding author to provide phone: +91 80 2293 2742; fax: +91 80 2360 0563; e-mail: r.bobbi@ece.iisc.ernet.in).

World Academy of Science, Engineering and Technology
International Journal of Biomedical and Biological Engineering
Vol:5, No:9, 2011

the activity of restorative parasympathetic system [41]. This increased parasympathetic activity has also been assessed through the slowing down of basal heart rate in meditators [42], and the increased synchronization, or respiratory sinus arrhythmia (RSA), between the breathing cycle and the heart beat during meditation [43], [44]. The RSA corresponds to high variability in heart rate as heart rate becomes faster during inhalation and slower during exhalation. Slow breathing has also been associated with increased baroreflex sensitivity [45], [46]. Decrease in blood pressure is often reported after meditation practice in both healthy subjects and hypertensive patients [47], [48]. Improved control of blood pressure is usually considered as a sign of balance between parasympathetic and sympathetic activity.

The analysis of heart rate variability (HRV), the variation of period between consecutive heart beats, provides valuable information to assess the autonomous nervous system (ANS). The HRV can be significantly affected by physiological state changes and many disease states. Hence, HRV analysis is becoming a major experimental and diagnostic tool. Its low cost, noninvasive nature and effectiveness encourages the development of new HRV analysis methods to broaden and improve its applications.

The analysis of HRV is not an easy task due to its nonstationarity [49]-[51] and nonlinearity [52]-[54] nature of time series. Traditional HRV analysis methods are based on linear methods in the time, frequency, or time-frequency domain. And these methods have been extensively used to reveal fundamental control activity of sympathetic and parasympathetic activity of ANS. The spectral analysis has led to the identification of three fairly distinct spectral peaks: high (0.15-0.5 Hz), low (0.05-0.15 Hz), and very low (0-0.05 Hz) frequency bands. The very low frequency (VLF) band has been associated with thermoregulation [55], low frequency (LF) spectral power reflects sympathetic and vagal influences on cardiac control via baroreceptor-mediated regulation of blood pressure [56]. The high frequency (HF) power is a function of respiratory modulation of vagal activity [41].

Many researchers have stressed on the importance of nonlinear techniques to study HRV [57]. This is because the cardiovascular system appears to be influenced by internal dynamics as well as from various external factors, which makes the system more dynamic and nonlinear. Generally, nonlinear dynamical analysis of time series involves estimation of dynamical invariants from the reconstructed attractor, such as, dimensions, Lyapunov exponents, and degree of nonlinearity. The classical nonlinear dynamical methods, such as correlation dimension [58], Lyapunov exponents [59], Poincare plots [60], various entropy measures [61]-[63], etc., have been used to quantify HRV dynamics. Several recent studies have used other nonlinear measures, including fractal dimension [64], approximate entropy [65], measures derived from symbolic dynamics and 1/f scaling [66], [67] to characterize HRV time series.

Many algorithms have been proposed in the literature to estimate nonlinear dynamical parameters from experimental time series data. However, most of these require long time series to obtain reliable estimates of nonlinear measures. In real biological systems, including while practicing meditation, acquiring long stationary time series may not be possible due to various reasons. Hence, the methods which give robust estimation results for shorter data lengths are very much desirable.

The nonlinear techniques, as mentioned above, have been widely used to study ANS in health as well as in various diseases. However, these methods have not been applied to study HRV during meditation. Even though there are some studies of HRV during meditation, those use linear spectral analysis techniques. These investigations have revealed that during meditation practices, there has been extremely prominent heart rate oscillations correlated with slow breathing [6], with amplitudes significantly greater than that measured before meditation, in the same individuals.

In this paper, we discuss application of nonlinear dynamical techniques to quantify HRV time series derived during meditation. Major emphasis is made on two types of mediation techniques; Chi meditation (Chinese style) [90] and Kundalini Yoga meditation (Indian style) [91]. We compute minimum embedding dimension, correlation dimension, largest Lyapunov exponent, and nonlinearity scores, from the HRV time series of both meditation and control (pre-meditation) state. We also aim to test the hypothesis that the nonlinear measures of HRV during meditation state would differ from those of control state.

II. MATERIALS AND METHODS

A. Minimum Embedding Dimension

The first step in nonlinear dynamical analysis is reconstruction of attractor in the phase space, from scalar time series. For this purpose, Taken's embedding theorem is used, which ensures reconstructed attractor to preserve all topological properties of the original attractor. If x_i, $i = 1, 2, ..., N$ is the time series, then the time delay vectors in phase space are formed as $y = [y_1, y_2, ..., y_L]^T$, where the number of time delay vectors are $L = N - (m-1)\tau$, and each time delay vector is expressed as $y_i = (x_i, x_{i+\tau}, ..., x_{i+(m-1)\tau})$, $i = 1, 2, ..., N - (m-1)\tau$, where m is the embedding dimension and τ is the time delay.

Proper reconstruction of the attractor is guaranteed if the dimension of the phase space is sufficient to unfold the attractor. It is shown that an embedding dimension of $m > 2d + 1$ will achieve this [68], where d is the dimension of the attractor. In most cases of the observed time series analysis, one neither has knowledge of d or m. There are many algorithms in the literature to estimate these quantities [69]-[73]. However, most of them have disadvantage of either being too subjective or computationally intensive. The method

World Academy of Science, Engineering and Technology
International Journal of Biomedical and Biological Engineering
Vol:5, No:9, 2011

proposed in [74] overcomes these difficulties and is suitable for short length time series also. More over, the method gives more reliable estimate of minimum embedding dimension (MED) even while the dimension of the system under consideration is sufficiently large.

The scalar time series is embedded in m-dimensional phase space, and the nearest neighbor for each phase space vector $y_i(m)$ is found and its distance in both dimensions m and $m+1$ are computed. The ratio of this distance is expressed as

$$a(i,m) = \frac{\left\| y_i(m+1) - y_{n(i,m)}(m+1) \right\|}{\left\| y_i(m) - y_{n(i,m)}(m) \right\|},$$

$i = 1, 2, ..., N - m\tau$, where $\|.\|$ denotes some measurement of Euclidian distance. In this analysis we have used maximum norm which is defined as $\left\| y_k(m) - y_l(m) \right\| = \max_{0 \le j \le m-1} \left| x_{k+j\tau} - x_{l+j\tau} \right|$. The $y_i(m+1)$ is the ith reconstructed vector with embedding dimension $m+1$. The $n(i,m)$ is an integer in the range $(1 \le n(i,m) \le N - m\tau)$ such that $y_{n(i,m)}(m)$ is the nearest neighbor of $y_i(m)$ in the m-dimensional reconstructed phase space, in the sense of distance $\|.\|$. The $n(i,m)$ depends on i and m. If $y_{n(i,m)}(m)$ equals $y_i(m)$, then the second nearest neighbor is taken.

If m is qualified as an embedding dimension according to the embedding theorem, then any two points which stay close in the m-dimensional reconstructed space will be still close in the $m+1$ dimensional reconstructed space. Such a pair of points is called true neighbors, otherwise they are false neighbors. Perfect embedding means that no false neighbors exist. Then the following quantity which is the mean value of all $a(i,m)$ is computed as $E(m) = \frac{1}{N - m\tau} \sum_{i=1}^{N-m\tau} a(i,m)$. The $E(m)$ is dependent only on the dimension m and the lag τ. To investigate its variation form m to $m+1$, we compute $E1(m) = \frac{E(m+1)}{E(m)}$. The $E1(m)$ stops changing when m is greater than some value m_0, if the time series comes from an attractor. Then $m_0 + 1$ is the minimum embedding dimension which accommodates the attractor completely. The saturation characteristics of $E1(m)$ is one indicator of presence of chaos in the time series.

For random time series $E1(m)$ will never attain a saturation value as m is increased. However, because of limited data samples and practical computations, it may be difficult to assess whether $E1(m)$ is slowly changing or stopped changing. In such situations, another quantity which is useful in distinguishing deterministic signals from stochastic signals is as $E^*(m) = \frac{1}{N - m\tau} \sum_{i=1}^{N-m\tau} \left| x_{i+m\tau} - x_{n(i,m)+m\tau} \right|$. Its variation from m to $m+1$ is computed as $E2(m) = \frac{E^*(m+1)}{E^*(m)}$. Since for random data future values are independent of past values, $E2(m)$ will be equal to 1 for any m, whereas for deterministic signals, there exist some m such that $E2(m) \ne 1$. It is advisable to determine both $E1(m)$ and $E2(m)$ to ensure presence of chaos. In the present study, we compute value of both of the quantities from epochs of HRV time series. The algorithm is particularly chosen because it is robust against length of time series, and gives reasonably good estimation even for high dimensional systems.

B. Correlation Dimension

The correlation dimension (CD) gives an estimate of system complexity. A dynamical system having strange attractor will have non-integer value for CD. Grassberger and Procaccia (GP) proposed an algorithm to compute CD from scalar time series [70], [75]. The disadvantage of GP algorithm is that it assumes the data is generated by a finite dimensional attractor and then seeks to determine its dimension. Hence, we almost always expect to get a finite fractional CD estimate from this algorithm. There are other methods to estimate correlation dimension based on kernel algorithms [76], [77].

Let $\{y_t\}_{t=1}^{L}$ be an embedding of a time series $\{x_i\}_{i=1}^{N}$ in $\Box^m$. The correlation function is defined by $C_L(\varepsilon) = \binom{L}{2}^{-1} \sum_{0 \le i < j \le L} I(\left\| y_i - y_j \right\| < \varepsilon)$, where $I(q)$ is the indicator function, which has a value of 1 if condition q is satisfied and 0 otherwise, and $\|.\|$ is distance function in $\Box^m$. The sum $\sum_i I(\left\| y_i - y_j \right\| < \varepsilon)$ is the number of points within a distance ε of y_j. If the points y_i are distributed uniformly within an object, this sum is proportional to volume of intersection of a sphere of radius ε with the object, and $C_L(\varepsilon)$ is proportional to the average of such volumes. Then $C_L(\varepsilon) \propto \varepsilon^{d_c}$, where d_c is the dimension of the object. Then the CD is defined as $d_c = \lim_{\varepsilon \to 0} \lim_{L \to \infty} \frac{\log C_L(\varepsilon)}{\log \varepsilon}$. Since the observation time series $\{x_i\}_{i=1}^{N}$ are contaminated by noise, one cannot know $\{y_t\}_{t=1}^{L}$ precisely. Therefore, computation

World Academy of Science, Engineering and Technology
International Journal of Biomedical and Biological Engineering
Vol:5, No:9, 2011

of $I(\|y_i - y_j\| < \varepsilon)$ is actually somewhat fuzzy. One can replace the hard indicator function with a continuous one, such as Gaussian basis functions $\exp\left(\dfrac{-\|y_i - y_j\|^2}{4\varepsilon}\right)$. The method is called Gaussian kernel algorithm. The generalization of correlation integral is as follows:

$$T_L^{d_e}(h) = \frac{1}{L} \sum_{0 \le i \le L} \left(\frac{1}{L-1} \sum_{0 \le j \ne i \le L} \exp\left(\frac{-\|y_i - y_j\|^2}{4h^2} \right) \right),$$

where h is analogous to ε, d_e is the embedding dimension. It is possible to use any other functions $\varphi(.)$ as kernel function, provided they should have finite (bounded) support. For any such function, it can be shown that the following correlation dimension scaling law holds $T_L^{d_e}(h) \propto h^{d_c}$. By using $\varphi(q) = \exp(-q^2/4)$, we get

$$T_L^{d_e}(h) \approx \varphi\left(\frac{h^2}{h^2 + \sigma^2} \right)^{d_e} e^{-K\tau d_e} \left(\frac{h^2 + \sigma^2}{d_e} \right)^{d_c/2}, \quad \text{when}$$

$\sqrt{h^2 + \sigma^2} \to 0$ and $d_e \to \infty$. In the above equation K is the correlation entropy, τ is the time delay. The noise level $\sigma = \sigma_n / \sigma_s$, where σ_n is the standard deviation of the additive Gaussian noise in the signal, and σ_s is the standard deviation of the observed signal (including the noise component). If $\sigma > 0$, $\sqrt{h^2 + \sigma^2} \to 0$ does not hold. By estimating $T_L^{d_e}(h)$ for a range of embedding dimensions d_e, one can estimate each of the parameters d_c, K, and σ, simultaneously. This is relatively robust technique which correctly accounts for noise when the noise is Gaussian and additive. This method is although technically more complex, in practice, more reliable and less prone to misinterpretation. We have computed CDs of epochs of HRV time series for various values of embedding dimension, and compared the values for pre-meditation and meditation states.

C. Measure of Predictability

Lyapunov exponents (LE) are used to characterize attractor of a dynamical system. The LEs quantify sensitivity of the system to initial conditions and are related to average rate of divergence or convergence of nearby trajectories in phase space. An m-dimensional dynamical system has m LEs, of which some of them may be positive. The set of all LEs is called Lyapunov spectrum, and presence of positive LE is an indication of chaos. However, a completely predictable system (such as periodic signals, etc) has zero LE, whereas chaotic systems have at least one positive LE. In most of the applications, it is sufficient to estimate only largest LE (LLE)

instead of Lyapunov spectrum. The LLE gives an idea about prediction zone of the time series under consideration.

Computing Lyapunov spectrum or LLE is straight forward when differential equations governing the system are known. However, in experimental set up, the governing equations of the system are not known, and one has only observation time series of the experiment. Wolf et al [78] proposed a method to estimate LLE. However, the method has a deficiency of orientational problem, since one has to successively replace nearby orbits, minimizing the orientational change. The method proposed by Sato et al [79] and is further improved by Rosenstein et al [80, overcome some of these problems.

After reconstruction of the attractor dynamics in a phase space, the number of phase space points is $L = N - (m-1)\tau$. The algorithm locates the nearest neighbor of each point on the trajectory. The nearest neighbor, $y_{\hat{i}}$, is found by searching for the point that minimizes the distance to the particular reference point, y_i. That is $d_j(0) = \min_{y_{\hat{i}}} \|y_i - y_{\hat{i}}\|$, where $d_j(0)$ is the initial distance from the jth point to its nearest neighbor, and $\|.\|$ denotes the Euclidian norm.

An additional constraint is imposed that nearest neighbors have a temporal separation greater than the mean period of the time series. That is $|j - \hat{j}| > mean \; period$. The mean period can be computed from the power spectrum as the reciprocal of mean frequency. Each pair of neighbors is considered to be nearby initial conditions for different trajectories. Then the LLE is estimated as mean rate of separation of the nearest neighbors.

$$\lambda_1(i) = \frac{1}{i\Delta t} \frac{1}{L-i} \sum_{j=1}^{L-i} \ln \frac{d_j(i)}{d_j(0)}, \quad \text{where} \quad \Delta t \quad \text{is the}$$

sampling period of the time series, $d_j(i)$ is the distance between j^{th} pair of nearest neighbors after i discrete time steps ($i\Delta t$ sec), and L is the number of phase space points. Since the equation converges slowly, then an alternate form is proposed.

$$\lambda_1(i,k) = \frac{1}{k\Delta t} \frac{1}{L-k} \sum_{i=1}^{L-k} \ln \frac{d_j(i+k)}{d_j(i)}, \quad k \text{ is} \quad \text{held}$$

constant, and λ_1 is estimated by looking the plateau region of $\lambda_1(i,k)$ with respect to i. This location of plateau is some times problematic and very subjective and hence estimated λ_1 is unreliable many times. This difficulty is due to the normalization of $d_j(i)$.

In general, the LLE can be defined using the equation $d(t) = Ce^{\lambda_1 t}$, where $d(t)$ is the average divergence at time

World Academy of Science, Engineering and Technology
International Journal of Biomedical and Biological Engineering
Vol:5, No:9, 2011

t and C is a constant that normalizes the initial separation. If the jth pair of neighbors diverge approximately at a rate given by the largest LE, then $d_j(i) \approx C_j e^{\lambda_1(i\Delta t)}$, where C_j is the initial separation. By taking log of both sides of this equation, we get $\ln d_j(i) \approx \ln C_j + \lambda_1(i\Delta t)$. This equation represents a set of approximately parallel lines (for $j = 1, 2, ..., L$), each with slope approximately proportional to λ_1. The average line can be defined by $z(i) = \frac{1}{\Delta t}\langle \ln d_j(i) \rangle$, where $\langle . \rangle$ denotes average over all values of j. The LLE is estimated using a least-square fit to this average line. This process of averaging helps to calculate accurate values of λ_1 using small, noisy time series. The LLE λ_1 is extracted from a least square fit to the longest possible linear region of $z(i)$ versus i plot. The presence of smooth linear region indicates positive LE.

The method is easy to implement, and computationally fast because it uses a simple measure of exponential divergence. This method gives more accurate values even for small data sets because it takes advantage of all the available data. The time evolution of logarithmic divergence is calculated and slope of the scaling region (LLE) is computed from epochs of HRV time series for both pre-meditation and meditation states.

D.Measure of Nonlinearity

Detection of nonlinearity in a time series needs a check for the presence of nonlinear time correlations among the time series values. The algorithm used in this study is based on the analysis of the extrema in time series. The theoretical and numerical results suggest that the sequence of extrema of a time series contains dynamical information on the process responsible for its generation.

It has been shown that a polar singularity corresponds to each local maximum or local minimum of the real time solution. Regular distribution of singularities reflects the corresponding periodic behavior of the real time solution [81]. The second condition arises from the general property of a stochastic process, which states that given a mean square differentiable stochastic process $w(t)$, the expected number of its extrema for unit time is contained in the joint density function of $w(t)$, $w'(t)$, and $w''(t)$ [82]. If the system is in a chaotic regime, then the corresponding sequence of singularities in the complex time plane associated with the local extrema becomes very irregular. It was also shown that the distances of these singularities from the real time axis, that is the position of these extrema are related to real values of the solution [83], [84].

The two algorithms proposed by Di Garbo et al extract these features such as number of extrema and length of broken line connecting these extrema as suitable statistics. The pattern of singularities in the complex time plane (PSC) algorithm uses length of broken line connecting these extrema. The number of extrema for unit time (NET) algorithm uses number of extrema in the unit time as statistics. Then, surrogate test is performed based on these statistics on extrema to account for Gaussian linear stochastic process. The significance of the test gives an estimation of its deviation from linearity. The procedure of nonlinearity test involves measurement of the above mentioned statistics for both original and surrogate data followed by statistical discrimination between them.

A larger value of nonlinear score means system is more nonlinear or it is deviating from a linear process which share many properties of system under consideration like mean, standard deviation, autocorrelation, and power spectrum, by a greater extent. We make use of methods proposed by [85].

Two types of surrogates are used in this analysis, Gaussian scaled (GS) and phase randomized (PR) surrogates [86]. The GS surrogates preserve histogram of amplitudes and approximately, the linear time correlations of the original time series. The PR surrogates preserve autocorrelation function and hence power spectrum. The steps involved in generating GS surrogates of time series are: (i) histogram transformation, (ii) Fast Fourier transform (FFT), (iii) phase randomization, (iv) inverse FFT, (v) inverse histogram transformation. However, in generating PR surrogates, only steps (ii) to (iv) are used.

In the PSC algorithm, the local maxima of the given time series are located and length of the line connecting these maxima is computed. The significance is computed as

$S_{psc} = \frac{|L - L_s|}{\sigma_s}$, where L is the broken length

corresponding to original and L_s is the mean of the broken line lengths $L_s(i)$, $i = 1, 2, ..., M$ corresponding to M surrogates, and σ_s is the standard deviation of lengths $L_s(i)$. In the NET algorithm, number of extrema for unit time in both original and surrogate time series is determined, and the statistic is computed as

$S_{net} = \frac{|N_o - N_s|}{\sigma_s}$, where N_o is the number of extrema in

the original signal and N_s is the mean of $N_s(i)$, $i = 1, 2, ..., M$ corresponding to number of extrema in the surrogate set, and σ_s is the standard deviation of $N_s(i)$. The values of S_{psc} and S_{net} for both GS and PR surrogates are computed. Both PSC and NET algorithms are used to calculate NLS of epochs of HRV time series, considering both Gaussian scaled and phase randomized surrogates. This has been done for pre-meditation and meditation states of both Chi and Kundalini systems of meditation.

World Academy of Science, Engineering and Technology
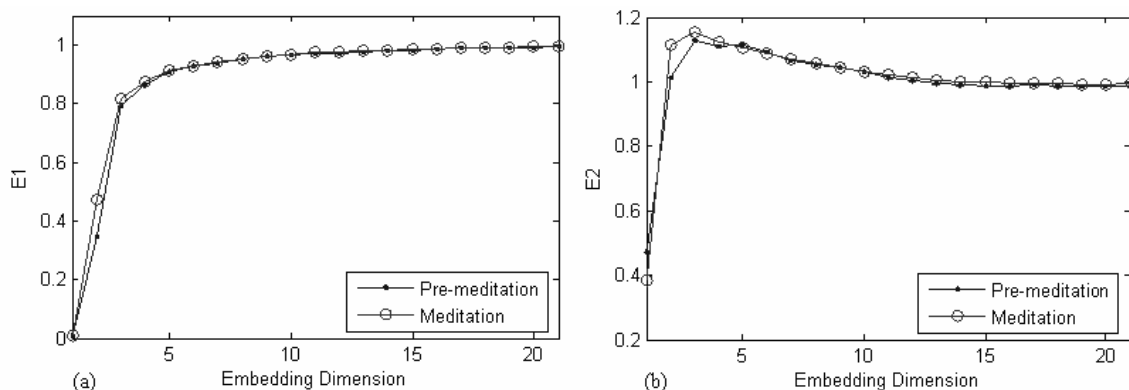International Journal of Biomedical and Biological Engineering
Vol:5, No:9, 2011

Fig. 1. Calculation of minimum embedding dimension (MED) values of HRV time series, the values E1 and E2 are plotted against the embedding dimension, for pre-meditation and meditation conditions of Chi meditation. The plot shows presence of chaos in HRV during Chi meditation.
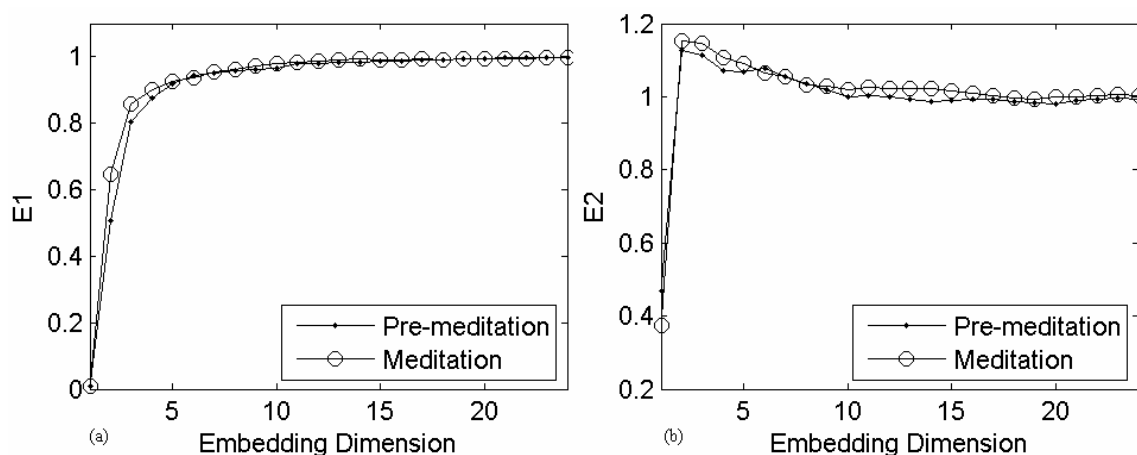

Fig. 2. Calculation of minimum embedding dimension (MED) values of HRV time series, the values E1 and E2 are plotted against the embedding dimension, for pre-meditation and meditation conditions of Kundalini meditation. The plot shows presence of chaos in HRV during Kundalini meditation.

E. Subjects and Meditation Protocols

In this study, two meditation techniques have been studied; (i) Chinese Chi meditation and (ii) Kundalini Yoga meditation. The meditation practitioners of both groups were in good general health, and they did not follow any specific exercise routines. From the 8 Chi meditators (5 females and 3 males, age range 26-35 years, mean age 29 years), 10 hours of Holter ECG recordings have been obtained. Each of the practitioners practiced one hour of meditation. During this session, they sat quietly, listening to the taped guidance of the Yoga Master. They were instructed to breathe spontaneously, while visualizing the opening and closing of a perfect lotus in the stomach. The meditation session lasted for about one hour. The 4 Kundalini Yoga meditators (2 females and 2 males, age range 20-52 years, mean age 33 years), wore Holter monitor for one and a half hours. 15 minute of base line quiet breathing were recorded before the one hour of meditation. The meditation protocol consisted of a sequence of breathing and chanting exercises, performed while seated in a cross legged posture.

Practitioners, in good general health condition, have been selected and ECG signals are recorded. The Holter recordings have been manually verified, and outliers deleted. The data is grouped into pre-meditation control and meditation, and is available online in the PhysioNet data archives [6]. Instantaneous heart rate time series are derived by taking the inverse of each successive inter beat intervals.

Prior to the analysis, all HRV time series are made uniformly sampled to have 4 samples per second, using cubic spline interpolation technique, and then digitally filtered with a band pass filter of 0.01-0.57 Hz, in order to remove high frequency noise which is out of the band of interest. The pre-processed HRV time series are then segmented into 3 minute epochs (3x60x4 = 720 samples), and then each of the epochs are subjected to nonlinear dynamical analysis. The nonlinear dynamical nature of HRV epochs is verified using Cao's method, and then nonlinear dynamical measures, such as correlation dimension, LLE, and nonlinearity scores are estimated for each of the epochs and averaged over the entire length of HRV time series. The extracted parameter values are group tested for statistical significance. Normal distribution of the values of nonlinear measures is assessed using the Shapiro-Wilks test for normality. Since many of the parameter values are non-normally distributed, comparison of nonlinear parameter values between meditation and pre-meditation

World Academy of Science, Engineering and Technology
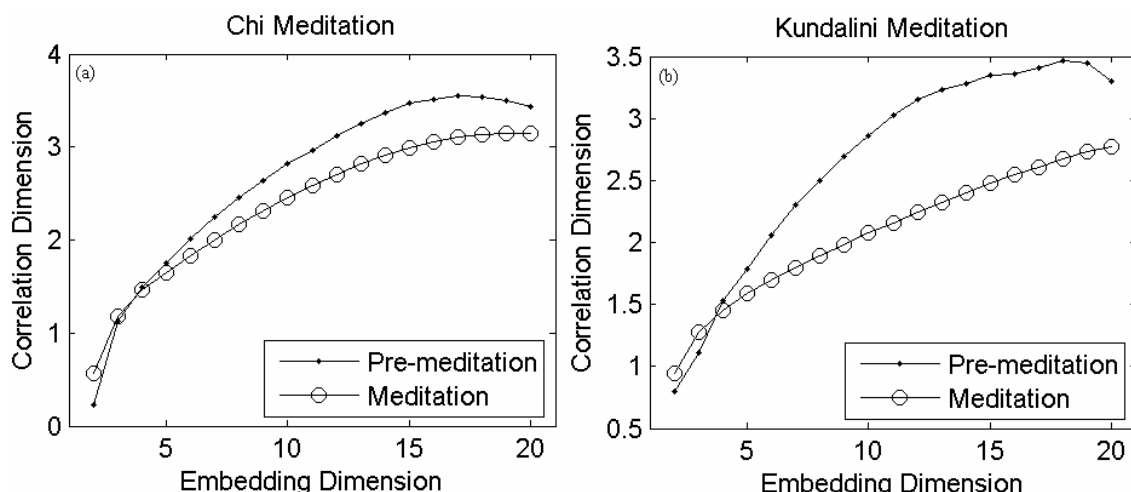International Journal of Biomedical and Biological Engineering
Vol:5, No:9, 2011

Fig. 3. Correlation dimension (CD) of HRV time series computed using Gaussian kernel algorithm, after embedding the series using different embedding dimensions. The CDs are computed for pre-meditation and meditation conditions of (a) Chi meditation, and (b) Kundalini meditation.

control is carried out using Kruskal-Wallis test, and a probability value of 0.05 is accepted as significant, and marked as 'a' in the tables.

III. RESULTS

The parameters E1 and E2 are computed from the epochs of HRV time series and averaged across the subjects, for each of the meditation cases. The variation of parameters E1 and E2 with respect to embedding dimension are shown in Fig. 1 and 2, respectively, for Chi and Kundalini meditation. It is clear from the figures that the parameter values attain saturation for higher values of embedding dimension. From the Fig. 1(a) and 2(a), it is clear that irrespective of the meditation type, the MED value reaches a constant value which can be taken 5, for both pre-meditation and meditation states. Looking at the values of E2 from the Fig. 1(b) and 2(b), E2 is not constant for all embedding dimension, and there are many embedding dimensions for which the value of E2 is not equal to one, indicating the chaotic nature of HRV time series under consideration.

Table 1 summarizes the CD values (mean, SD), for pre-meditation and meditation states and the p-values of Kruskal-Wallis test, for Chi meditation. The same is depicted in the Table 2 for the case of Kundalini meditation. The average value of CD is plotted for various embedding dimensions in Figure 3. The pre-meditation state has lower CD values than the meditation state, for embedding dimensions greater than 4, with significant differences between the two states. The result suggests that the HRV during meditation state is less complex than during control state.

In order to estimate LLE, the time evolution of log of divergence is plotted as shown in Fig. 4. The box plot of estimated LLEs is shown in Fig. 5, and results are summarized in the Table 3. There is a significant increase in the value of LLE for meditation state compared to pre-meditation state,

TABLE I
AVERAGE CORRELATION DIMENSION VALUES IN VARIOUS EMBEDDING
DIMENSIONS FOR HRV TIME SERIES OF CHI MEDITATION

	Pre-meditation		Meditation		Statistical analysis	
ED	mean	std	mean	std	Chi-sq	p-value
2	0.2333	0.8399	0.5711	0.7290	2.8235	0.0928
3	1.1298	0.0555	1.1779	0.0421	3.1875	0.0742
4	1.4964	0.0494	1.4610	0.0896	0.3970	0.5286
5	1.7495	0.0581	1.6519	0.1166	2.8235	0.0928
6	2.0152	0.0835	1.8328	0.1667	5.3382	0.0208a
7	2.2421	0.1093	2.0010	0.2106	5.3382	0.0208a
8	2.4560	0.1289	2.1643	0.2570	5.8346	0.0157a
9	2.6425	0.1338	2.3117	0.2812	5.8346	0.0157a
10	2.8158	0.1239	2.4500	0.3002	5.3382	0.0208a
11	2.9699	0.1365	2.5827	0.3168	5.3382	0.0208a
12	3.1153	0.1384	2.7051	0.3238	6.3529	0.0117a
13	3.2549	0.1463	2.8170	0.3245	7.4559	0.0063a
14	3.3744	0.1591	2.9159	0.3173	8.6471	0.0032a
15	3.4659	0.1718	2.9935	0.2962	8.6471	0.0032a
16	3.5166	0.1729	3.0542	0.2715	8.0404	0.0045a
17	3.5535	0.1858	3.1026	0.2415	9.2757	0.0023a
18	3.5382	0.1832	3.1390	0.2093	8.6471	0.0032a
19	3.5002	0.1793	3.1499	0.1693	8.0404	0.0045a
20	3.4315	0.1532	3.1497	0.1359	8.0404	0.0045a

which states that the HRV time series during meditation is less predictable than that during pre-meditation state.

The nonlinearity scores (NLS) estimated from HRV time series using PSC and NET algorithms, considering both GS and PR surrogates, are shown in Table 4 and 5 respectively for Chi and Kundalini meditation. It is observed that the NLS are higher for meditation state than that for pre-meditation state. The results are significant in NET algorithm ($p < 0.05$). Even though, the NLS using Gaussian scaled PSC algorithm has not
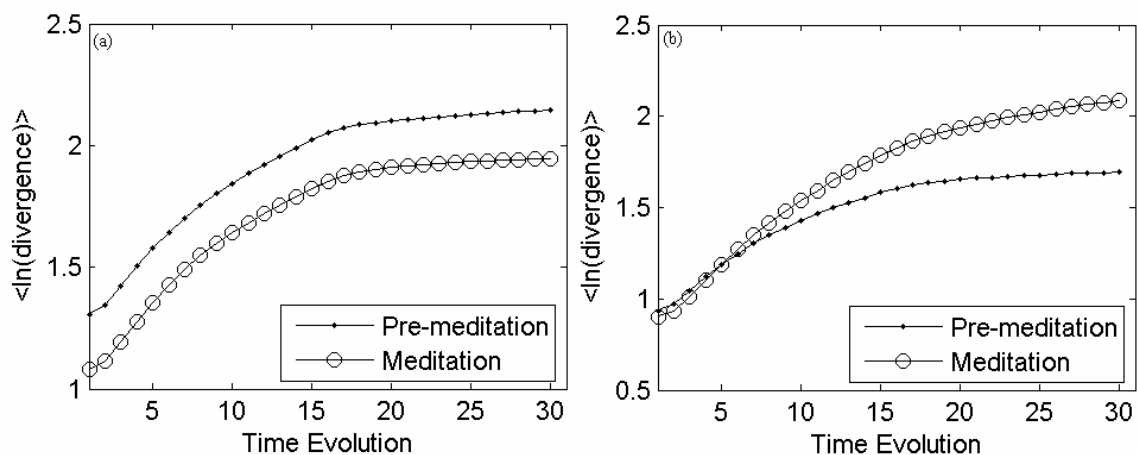
World Academy of Science, Engineering and Technology
International Journal of Biomedical and Biological Engineering
Vol:5, No:9, 2011

Fig. 4. Plot of <ln(divergence)> versus time to compute LLE of HRV time series. The LLE is estimated by calculating slope of the line after least square fit. The curves are shown for pre-meditation and meditation conditions of (a) Chi and (b) Kundalini meditation.
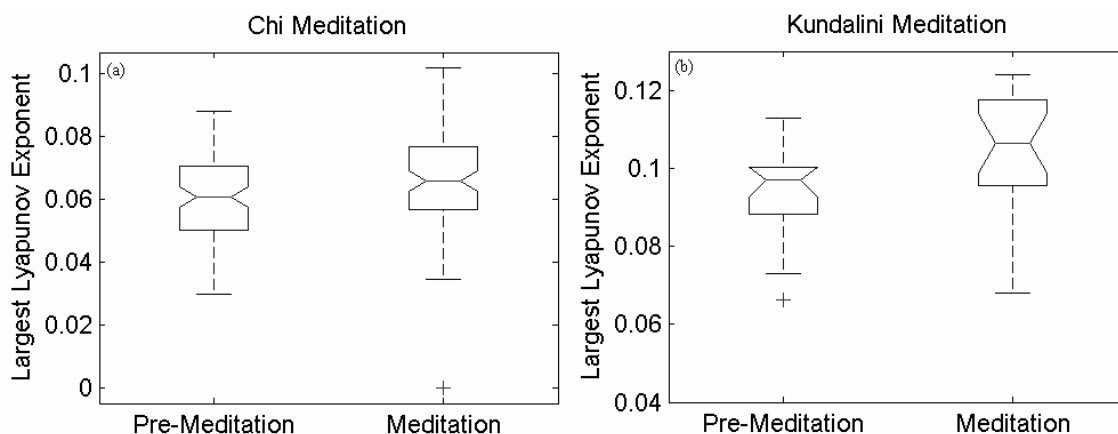

Fig. 5. Box-plot of LLE of HRV in pre-meditation and meditation conditions, (a) Chi meditation, (b) Kundalini meditation.

shown as much difference as for NET algorithm in the case of Kundalini meditation, the values are comparable.

IV. DISCUSSION

In this study, we have analyzed HRV time series, derived while performing two types of meditation practices, using nonlinear dynamic techniques. The meditation practices considered here are Chi meditation and Kundalini Yoga meditation. The nonlinear dynamic parameters such as NLS, MED, CD, and LLE are derived from the reconstructed attractor of scalar HRV time series. To compute these nonlinear dynamical parameters, we have chosen the methods, which are explained in the methods section, that give more accurate estimation results even for short length of time series.

The MED parameter is measured to check the nonlinear dynamical nature of HRV during meditation, which quantifies the interaction of dynamical parameters. In each of the meditation states, the attractor of the system can be reconstructed from time series with smaller embedding dimension compared to pre-meditation state. The MED values can be taken in the range 8-15 to completely unfold the dynamics. Even though there are not much difference in the

MED values of HRV between meditation and pre-meditation states, the results indicate high dimensional chaotic nature of HRV time series in both meditation and pre-meditation states.

The HRV during meditation has shown a higher value of NLS compared to pre-meditation state. Higher NLS have suggested an increased nonlinearity of HRV, especially in meditation state. The higher NLS probably reflect possible increase in sympathetic function during meditation. The differences in NLS between the two states are also statistically significant. The NLS measures used in this work are based on local extrema of time series.

The CD gives a measure of complexity of systems measured as degree of freedom or number of state variables of the dynamical system. It is found that during meditation state the HRV time series have significantly lower CD values than pre-meditation state. From this it is inferred that the HRV during meditation is more rhythmic. The reduction of irregularity of HRV could be explained by a decrease of dynamical complexity of cardiovascular system. The statistical analysis has showed that the CDs are best differentiable between the two groups.

World Academy of Science, Engineering and Technology
International Journal of Biomedical and Biological Engineering
Vol:5, No:9, 2011

TABLE II
AVERAGE CORRELATION DIMENSION VALUES IN VARIOUS EMBEDDING
DIMENSIONS FOR HRV TIME SERIES OF KUNDALINI MEDITATION

ED	Pre-meditation		Meditation		Statistical analysis	
	mean	std	mean	std	Chi-sq	p-value
2	0.7934	0.0763	0.9424	0.0233	5.3333	0.0209a
3	1.1121	0.0793	1.2744	0.0465	4.0833	0.0433a
4	1.5344	0.0907	1.4564	0.0397	3.0000	0.0832
5	1.7882	0.1094	1.5859	0.0548	5.3333	0.0209a
6	2.0565	0.1634	1.6937	0.0632	5.3333	0.0209a
7	2.2992	0.1926	1.7923	0.0720	5.3333	0.0209a
8	2.4983	0.2160	1.8888	0.0819	5.3333	0.0209a
9	2.6926	0.2532	1.9828	0.0911	5.3333	0.0209a
10	2.8612	0.2847	2.0734	0.0958	5.3333	0.0209a
11	3.0216	0.3242	2.1592	0.0966	5.3333	0.0209a
12	3.1486	0.3589	2.2433	0.0935	5.3333	0.0209a
13	3.2292	0.3691	2.3255	0.0872	5.3333	0.0209a
14	3.2792	0.3652	2.4033	0.0800	5.3333	0.0209a
15	3.3443	0.4018	2.4794	0.0822	5.3333	0.0209a
16	3.3591	0.4142	2.5460	0.0985	5.3333	0.0209a
17	3.4093	0.5233	2.6093	0.1302	5.3333	0.0209a
18	3.4661	0.7085	2.6742	0.1775	3.0000	0.0832
19	3.4506	0.7727	2.7305	0.2228	3.0000	0.0832
20	3.3023	0.6069	2.7760	0.2666	2.0833	0.1489

TABLE III
AVERAGE LLE OF HRV IN CHI MEDITATION

Pre-meditation		Meditation		Statistical analysis	
Mean	Std	Mean	Std	chi-sq	p-value
0.0603	0.0123	0.0639	0.0206	6.3403	0.0118a

TABLE IV
AVERAGE LLE OF HRV IN KUNDALINI MEDITATION

Pre-meditation		Meditation		Statistical analysis	
Mean	Std	Mean	Std	chi-sq	p-value
0.0900	0.0241	0.1034	0.0166	5.5383	0.0186a

The predictability of the system is quantified by LLE, which also gives the presence of chaos. The LLE describes the rate of exponential divergence of trajectories and sensitive dependence on the initial condition. During meditation state the HRV showed higher LLE which confirms decreased predictability in this state compared to pre-meditation state. The decrease in predictability (increase in LLE) probably reflects a high degree of chaos during meditation state compared to pre-meditation state. This can be due to increased nonlinear interaction of variables in meditation state, and may be related to increased sympathetic activity and changes in peripheral vascular mechanisms. It is also found that HRV time series are chaotic both before and during meditation, as suggested by the positive LLEs in either state.

The intense stimulation of either the sympathetic or parasympathetic system could ultimately result in simultaneous

TABLE V
AVERAGE NONLINEARITY SCORE OF HRV IN CHI MEDITATION

PSC Algorithm

	Pre-meditation		Meditation		Statistical analysis	
	mean	std	mean	std	Chi sq	p-value
PRS	1.9171	0.8352	4.3339	2.2337	5.8346	0.0157a
GSS	2.7662	0.6686	6.3246	2.5818	9.9265	0.0016a

NET Algorithm

	Pre-meditation		Meditation		Statistical analysis	
	mean	std	mean	std	Chi sq	p-value
PRS	2.1350	0.8524	4.3068	2.3547	3.5735	0.0587
GSS	3.4606	0.4634	5.0411	1.4517	6.3529	0.0117a

TABLE VI
AVERAGE NONLINEARITY SCORE OF HRV IN KUNDALINI MEDITATION

PSC Algorithm

	Pre-meditation		Meditation		Statistical analysis	
	mean	std	mean	std	Chi sq	p-value
PRS	1.2549	0.7801	3.1124	2.5697	4.3200	0.0377a
GSS	2.2256	1.8778	4.1634	3.3446	3.0000	0.0833

NET Algorithm

	Pre-meditation		Meditation		Statistical analysis	
	mean	std	mean	std	Chi sq	p-value
PRS	1.1921	0.5847	5.3436	2.6278	15.8700	0.0001a
GSS	2.6685	0.7476	6.3294	2.3294	14.5200	0.0001a

discharge of both systems [87], [97]. Several studies have demonstrated influence of autonomic activity during meditation associated with decreased heart rate and blood pressure, decreased respiratory rate, and decreased oxygen metabolism [88], [3], [10], [92], [93]. However, a recent study of meditative techniques suggested a mutual activation of parasympathetic and sympathetic systems by demonstrating an increase in the variability of heart rate during meditation [6]. The increased variation in heart rate was hypothesized to reflect activation of both arms of ANS. This notion is consistent with recent developments in the study of autonomic interactions [89] [94]-[96], and also fits the characteristic description of meditative states in which there is a sense of overwhelming calmness as well as significant alertness.

The present study of HRV time series using nonlinear techniques has shown significant differences between the pre-meditation and meditation states, and thus could give additional insight into underlying dynamics of HRV and in the investigation of cardiac autonomic function during meditation. However, it should be noted that the present study has been considered on a smaller sample size of data and further

World Academy of Science, Engineering and Technology
International Journal of Biomedical and Biological Engineering
Vol:5, No:9, 2011

investigation is required on a larger sample of data size to substantiate the present work.

REFERENCES

[1] Baer RA. Mindfulness training as a clinical intervention: a conceptual and empirical review. Clin Psychol Sci Pract 2003; 10: 125-143.

[2] Ospina MB, Bond TK, Karkhaneh M, Tjosvold L, Vandermeer B, Liang Y, Bialy L, Hooton N, Buscemi N, Dryden DM, Klassen TP. Meditation practices for health: state of the research. Evid Rep Technol Assess (Full Rep) 2007; 115: 1-263.

[3] Sudsuang R, Chentanez V, Veluvan K. Effects of Buddhist meditation on serum cortisol and total protein levels, blood pressure, pulse rate, lung volume and reaction time. Physiol Behav 1991; 50: 543-548.

[4] Wenneberg SR, Schneider RH, Walton KG, Maclean CR, Levitsky DK, Salerno JW, Wallace RK, Mandarino JV, Rainforth MV, Waziri R. A controlled study of the effects of the Transcendental Meditation program on cardiovascular reactivity and ambulatory blood pressure. Int J Neurosci 1997; 89: 15-28.

[5] Lehrer P, Sasaki Y, Saito Y. Zazen and cardiac variability. Psychosom Med 1999; 61: 812-821.

[6] Peng CK, Mietus JE, Liu Y, Khalsa G, Douglas PS, Benson H, Goldberger AL. Exaggerated heart rate oscillations during two meditation techniques. Int J Cardiol 1999; 70:101-107.

[7] Peng CK, Henry IC, Mietus JE, Hausdorff JM, Khalsa G, Benson H, Goldberger AL. Heart rate dynamics during three forms of meditation. Int J Cardiol 2004; 95:19-27.

[8] Lee MS, Kim BG, Huh HJ, Ryu H, Lee HS, Chung HT. Effect of Qi-training on blood pressure, heart rate and respiration rate. Clin Physiol 2000; 20: 173-176.

[9] Barnes VA, Treiber FA, Davis H. Impact of transcendental meditation on cardiovascular function at rest and during acute stress in adolescents with high normal blood pressure. J Psychosom Res 2001; 51: 597-605.

[10] Travis F. Autonomic and EEG patterns distinguish transcending from other experiences during transcendental meditation practice. Int J of Psychophysiol 2001; 42: 1-9.

[11] Young JDE, Taylor E. Meditation as a voluntary hypometabolic state of biological estivation. News in Pyusiological Sci 1998; 13: 149-153.

[12] Infante JR, Torres-Avisbal M, Pinel P, Vallejo JA, Peran F, Gonzalez F, Contreras P, Pacheco C, Roldan A, Latre JM. Catecholamine levels in practitioners of the transcendental meditation technique. Physiol Behav 2001; 72: 141-146.

[13] Wallace RK, Benson H, Wilson AF. A wakeful hypometabolic physiologic state. The Am J Physiol 1971; 221(3): 795-799.

[14] Jacobs GD, Friedman R. EEG spectral analysis of relaxation technique. Appl Psychophysiol Biofeedb 2004; 29: 245-254.

[15] Stetter F, Kupper S. Autogenic training: a meta-analysis of clinical outcome studies. Appl Psychophysiol Biofeedb 2002; 27: 45-98.

[16] Benson H, Beary JF, Carol MP. The relaxation response. Psychiatry 1974; 37: 37-46.

[17] Dillbeck MC, Orme-Johnson DW. Physiological differences between transcendental meditation and rest. American Psychologist 1987; 42: 879-881.

[18] Jones BM. Changes in cytokine production in healthy subjects practicing Guolin Qigong: a pilot study. BMC Complementary and Alternative Medicine 2001; 1: 8. online at: http://www.biomedcentral.com/1472-6882/1/8.

[18] Manjunath NK, Telles S. Influence of Yoga & Ayurveda on self-rated sleep in a geriantric population. Indian J of Medical Res 2005; 121: 683-690.

[20] Oman D, Shapiro SL, Thoresen CE, Plante TG, Flinders T. Meditation lowers stress and supports forgiveness among college students: a randomized controlled trial. J Am Coll Health 2008; 56: 569–578.

[21] Telles S, Reddy SK, Nagendra HR. Oxygen consumption and respiration following two yoga relaxation techniques. Appl Psychophysiol Biofeedback 2000; 25(4): 221–227.

[22] Sarang PS, Telles S. Oxygen consumption and respiration during and after two yoga relaxation techniques. Appl Psychophysiol Biofeedb 2006a; 31(2): 143-151.

[23] Sarang PS, Telles S. Effects of two yoga based relaxation techniques on heart rate variability (HRV). Int J Stress Manag 2006b; 13(4): 460-475.

[24] Vempati RP, Telles S. Baseline occupational stress levels and physiological responses to a two day stress management program. J Indian Psychol 2000; 18: 33-37.

[25] Harinath K, Malhotra AS, Pal K, Prasad R, Kumar R, Kain TC, Rai L, Sawhney RC. Effects of Hatha yoga and Omkar meditation on cardiorespiratory performance, psychologic profile, and melatonin secretion. J Alternative and Complementary Med 2004; 10: 261-268.

[26] Kirkwood G, Rampes H, Tuffrey V, Richardson J, Pilkington K. Yoga for anxiety: A systemic review of the research evidence. Br J Sports Med 2005; 39: 884-891.

[27] Malathi A, Damodaran A, Shah N, Krishnamurthy G, Namjoshi P, Ghodke S. Psychophysiological changes at the time of examination in medical students before and after the practice of yoga and relaxation. Indian J of Psychiatry 1998; 40: 35-40.

[28] Michalsen A, Grossman P, Acil A, Langhorst J, Ludtke R, Esch T, Stefano GB, Dobos GJ. Rapid stress reduction and anxiolysis among distressed women as a consequence of a three-month intensive yoga program. Med Sci Monitor 2005; 11: CR555-CR561.

[29] Manjunath NK, Telles S. Spatial and verbal memory test scores following yoga and fine arts camps for school children. Indian J Physiology and Pharmacology 2004; 48: 353-354.

[30] Ray US, Mukhopadhyaya S, Purkayastha SS, Asnani V, Tomer OS, Prasad R, Thakur L, Selvamurthy W. Effect of yoga exercises on physical and mental health of young fellowship course trainees. Indian J Physiology and Pharmacology 2001; 45: 37-53.

[31] Manjunath NK, Telles S. Improved performance in the Tower of London test following yoga. Indian J Physiology and Pharmacology 2001; 45: 351-354.

[32] Tran MD, Holly RG, Lashbrook J, Amsterdam EA. Effects of Hatha yoga practice on the health-related aspects of physical fitness. Preventive Cardiology 2001; 4: 165-170.

[33] Lou HC, Kjaer TW, Friberg L, Wildschiodtz G, Holm S. A ^{15}O-H2O PET study of meditation and the resting state of normal consciousness. Hum Brain Mapp 1999; 7(2): 98-105.

[34] Travis F, Pearson C. Pure consciousness: distinct phenomenological and physiological correlates of "consciousness itself". Int J Neurosci 2000; 100: 77-89.

[35] Newberg A, Alavi A, Baime M, Pourdehnad M, Santanna J, d'Aquili E. The measurement of regional cerebral blood flow during the complex cognitive task of meditation: A preliminary SPECT study. Psychiatr Res 2001; 106(2): 113-122.

[36] Gaylord C, Orme-Johnson D, Travis F. The effects of the transcendental meditation technique and progressive muscle relaxation on EEG coherence. Stress reactivity and mental health in black adults. Int J Neurosci 1989; 46: 77-86.

[37] Panjwani U, Gupta HL, Singh SH, Selvamurthy W, Rai UC. Effect of Sahaja Yoga practice on stress management in patients of epilepsy. Indian J Physiol Pharmacol 1995; 39: 111-116.

[38] Lee MS, Bae BH, Ryu H, Sohn JH, Kim SY, Chung HT. Changes in alpha wave and state anxiety during ChunDoSunBup Qi-training in trainees with open eyes. Am J Chinese Med 1997; 25: 289-299.

[39] Eckberg DL, Nerhed C, Wallin BG. Respiratory modulation of muscle sympathetic and vagal cardiac outflow in man. J Psychophysiol 1985; 356: 181-196.

[40] Badra LJ, Cooke WH, Hoag JB, Crossman AA, Kuusela TA, Tahvanainen KUO, Eckberg DL. Respiratory modulation of human autonomic rhythms. Am J Physiol- Heart and Circulatory Physiol 2001; 280: H2674-H2688.

[41] Saul JP. Beat-to-beat variations of heart rate reflect modulation of cardiac autonomic outflow. News in Psychological Sci 1990; 5: 32-37.

[42] Pal GK, Velkumary S, Madanmohan. Effect of short-term practice of breathing exercises on autonomic functions in normal human volunteers. Indian J Med Res 2004; 120: 115-121.

[43] Cysarz D, Bussing A. Cardiorespiratory synchronization during Zen meditation. Eur J Appl Physiol 2005; 95: 88-95.

[44] Ditto B, Eclache M, Goldman M. Short-term autonomic and cardiovascular effects of mindfulness body scan meditation. Ann Behav Med 2006; 32: 227-234.

[45] Joseph CN, Porta C, Casucci G, Casiraghi N, Maffeis M, Rossi M, Bernardi L. Slow breathing improves arterial baroreflex sensitivity and decreases blood pressure in essential hypertension. Hypertension 2005; 45: 714-718.

World Academy of Science, Engineering and Technology
International Journal of Biomedical and Biological Engineering
Vol:5, No:9, 2011

[46] Reyes Del Paso GA, Cea JI, González-Pinto A, Cabo OM, Caso R, Brazal J, Martínez B, Hernández JA, González MI. Short-term effects of a brief respiratory training on baroreceptor cardiac reflex function in normotensive and mild hypertensive subjects. Appl Psychophysiol Biofeedback 2006; 31: 37-49.

[47] Carlson LE, Speca M, Faris P, Patel KD. One year pre-post intervention follow-up of psychological, immune, endocrine and blood pressure outcomes of mindfulness-based stress reduction (MBSR) in breast and prostate cancer outpatients. Brain Behav Immun 2007; 21: 1038-1049.

[48] Manikonda JP, Störk S, Tögel S, Lobmüller A, Grünberg I, Bedel S, Schardt F, Angermann CE, Jahns R, Voelker W. Contemplative meditation reduces ambulatory blood pressure and stress-induced hypertension: a randomized pilot trial. J Hum Hypertens 2008; 22: 138-140.

[49] Zebrowski JJ, Baranowski R. Nonlinear instabilities and nonstationarity in human heart rate variability. IEEE Comput Sci Eng 2004; 6: 78-83.

[50] Hoyer D, Schmidt K, Bauer R, Zwiener U, Kohler M, Luthke B, Eiselt M. Nonlinear analysis of heart rate and respiratory dynamics. IEEE Eng Med Biol Mag 1997; 16: 31-39.

[51] Webber CL, Zbilut JP. Dynamical assessment of physiological system and states using recurrence plot strategies. J Appl Physiol 1994; 76: 965-973.

[52] Goldberger AL, Rigney DR, West BJ. Chaos and fractals in human physiology. Sci Am 1990; 262: 42-49.

[53] Poon CS, Merrill CK. Decrease of cardiac chaos in congestive heart failure. Nature 1997; 2: 389.

[54] Zbilut JP, Santucci PA, Yang SY, Podolski JL. Linear and nonlinear evaluation of ventricular arrhythmias. Proc ISMDA 2002; 151-157.

[55] Kitney RI. An analysis and simulation of the human thermoregulatory control system. Med Biol Eng 1974; 12: 56-64.

[56] Pagani M, Rimoldi O, Malliani A. Low-frequency components of cardiovascular variabilities as markers of sympathetic modulation. Trends Pharmacol Sci 1992; 13: 50-54.

[57] Goldberger AL, West BJ. Fractals in physiology and medicine. Yale J Biol Med 1987; 60: 421-435.

[58] Carvajal R, Wessel N, Vallverdu M, Caminal P, Voss A. Correlation dimension analysis of heart rate variability in patients with dilated cardiomyopathy. Comput Meth Progr Biomed 2005; 78: 133-140.

[59] Kim WS, Yoon YZ. Nonlinear characteristics of heart time series: influence of three recumbent positions in patients with mild or severe coronary artery disease. Physiol Meas 2005; 26: 517-529.

[60] Kamen PW, Krum H, Tonkin AM. Poincare plot of heart rate variability allows quantitative display of parasympathetic nervous activity in humans. Clin Sci (London) 1996; 91: 201-208.

[61] Costa M, Goldberger AL, Peng CK. Multiscale entropy analysis of biological signals. Phys Rev E 2005; 71: 021906-1-021906-18.

[62] Lake DE, Richman JS, Griffin MP, Moorman JR. Sample entropy analysis of neonatal heart rate variability. Am J Physiol Regul Integr Comp Physiol 2002; 283: R789-R797.

[63] Lewis MJ, Short AL. Sample entropy of electrocardiographic RR and QT time-series data during rest and exercise. Physiol Meas 2007; 28: 731-744.

[64] Goldberger AL. Fractal variability versus pathologic predictability: complexity loss and stereotypy in disease. Perspect Biol Med 1997; 40: 543-561.

[65] Storella RJ, Wood HW, Mills KM, Kanters JK, Højgaard MV, Holstein-Rathlou NH. Approximate entropy and point correlation dimension of heart rate variability in healthy subjects. Integr Psychol Behav Sci 1998; 33(4): 315-320.

[66] Meyer M, Stiedl O. Self-affine fractal variability of human heart beat interval dynamics in health and disease. Eur J Appl Physiol 2003; 90: 305-316.

[67] Iyenger I, Peng CK, Morin R. Age-related alterations in the fractal scaling of cardiac interbeat interval dynamics. Am J Physiol Regul Integr Comp Physiol 1996; 271: R1078-R1084.

[68] Takens F. Detecting strange attractors in turbulence. In Dynamical Systems and Turbulunce, vol 898, Lecture notes on Mathematics, Eds Rand D and Young L, Springer-Verlag, 1980; 366-381.

[69] Broomhead DS, King GP. Extracting qualitative dynamics from experimental data. Physica D1986; 20: 217–236.

[70] Grassberger P, Procaccia I. Measuring the strangeness of strange attractors. Physica D 1983a; 9: 189–208.

[71] Kennel MB, Brown R, Abarbanel HDI. Determining minimum embedding dimension using a geometrical construction. Phys Rev A 1992; 45: 3403–3411.

[72] Mees AI, Rapp PE, Jennings LS. Singular value decomposition and embedding dimension. Phys Rev A 1987; 37: 340–346.

[73] Theiler J. Efficient algorithm for estimating the correlation dimension from a set of discrete points. Phys Rev A 1987; 36: 4456–4462.

[74] Cao L. Practical method for determining the minimum embedding dimension of a scalar time series. Physica D 1997; 110: 43-50.

[75] Grassberger P, Procaccia I. Characterization of strange attractors. Phys Rev Lett 1983b; 50: 346–349.

[76] Diks C. Estimating invariants of noisy attractors. Phys Rev E 1996; 53: R4263-R4266.

[77] Yu D, Small M, Harrison RG, Diks C. Efficient implementation of the Gaussian kernel algorithm in estimating invariants and noise level from noisy time series data. Physical Rev E 2000; 61(4): 3750-3756.

[78] Wolf A, Swift J, Swinney H, Vastano J. Determining Lyapunov exponents from a time series. Physica D 1985; 16: 285–317.

[79] Sato S, Sano M, Sawada Y. Practical methods of measuring the generalized dimension and largest Lyapunov exponents in high-dimensional chaotic systems. Prog Theor Phys 1987; 77: 1-5.

[80] Rosenstein MT, Collins JJ, De Luca CJ. A practical method for calculating largest Lyapunov exponents from small data sets. Physica D 1993; 65: 117-134.

[81] Ramani A, Grammaticos B, Bountis T. The Painleve property and singularity analysis of integrable and nonintegrable systems. Physics Rep 1989; 180: 161.

[82] Soong TT. Random differential equations in science and engineering. Ed. Bellman R, 1973, Academic Press.

[83] Tabor M, Weiss J. Analytic structure of the Lorentz system. Phys Rev A 1981; 24: 2157–2167.

[84] Konno K, Tateno H. Duffing's equation in complex time and chaos. Prog Theor Phys 1984; 72: 1047–1049.

[85] Di Garbo A, Balocchi R, Chillemi S. Nonlinearity tests using the extrema of a time series. Int J Bifurcation Chaos 1998; 8: 1831–1838.

[86] Theiler J, Eubank S, Longtin A, Galdrikian B, Farmer JD. Testing for nonlinearity in time series: the method of surrogate data. Physica D 1992; 58: 77-94.

[87] Gellhorn E, Kiely WF. Mystical states of consciousness: neurophysiological and clinical aspects. J Nerv Mental Dis 1972; 154: 399-405.

[88] Jevning R, Wallace RK, Beidebach M. The physiology of meditation: a review. A wakefulness hypometabolic integrated response. Neurosci Biobehav Rev 1992; 16: 415-424.

[89] Hugdahl K. Cognitive influences on human autonomic nervous system function. Curr Opin Neurobiol 1996; 6: 252-258.

[90] Cheng TO. Tai Chi: The Chinese ancient wisdom of an ideal exercise for cardiac patients. Int J Cardiol 2007; 117:293-295.

[91] Arambula P, Peper E, Kawakami M, Gibney KH. The physiological correlates of Kundalini Yoga meditation: a study of a Yoga master. Appl Physiol Biofeedback 2001; 26(2): 147-153.

[92] Phongsuphap S, Phongsuphap Y, Chandanamattha P, Lursinsap C. Changes in heart rate variability during concentration meditation. Int J Cardiol 2008; 130:481-484.

[93] Telles S, Desiraju T. Autonomic changes in Brahmakumaris Raja Yoga meditation. Int J Psychophysiol 1993; 15: 147-152.

[94] Tang YY, Ma Y, Fan Y, Feng H, Wang W, Feng S, Lu Q, Hu B, Lin Y, Li J, Wang Y, Zhou L, Fan M. Central and autonomic nervous system interaction is altered by short-term meditation. Proc Nat Acad Aci USA 2009; May.

[95] Jerath R, Edry JW, Barnes VA, Jerath V. Physiology of long pranayamic breathing: Neural respiratory elements may provide a mechanism that explains how slow deep breathing shifts the autonomic nervous system. Med Hypoth 2006; 67: 566-571.

[96] Takahashi T, Murata T, Hamada T, Omori M, Kosaka H, Kikuchi M, Yoshida H, Wada Y. Changes in EEG and autonomic nervous activity during meditation and their association with personality traits. Int J of Psychophysiol 2005; 55: 199-207.

[97] Friedman EH, Coats AJS. Neurobiology of heart rate oscillations during two meditative techniques. Int J Cardiol 2000; 73:199.

B. S. Raghavendra was born in Bobbi-Thirthahalli, India. He received B.E. degree from Bangalore University in 2001, and M. Tech. degree in Electronics and Communication Engineering from National Institute of Technology Karnataka, Surathkal, India, in 2004. Currently he is pursuing his Ph.D. in the Department of Electrical Communication Engineering, Indian Institute of Science, Bangalore, India. His research interests include biomedical signal processing, nonlinear dynamics, and computational neuroscience.

D. Narayana Dutt obtained his Ph.D degree in Electrical Communication Engineering from the Indian Institute of Science, Bangalore, India. He has been a member of faculty in the same Institute for the past several decades. He worked earlier in the areas of acoustics and speech signal processing. He has been working for the past several decades in the area of applications of digital signal processing to the analysis of biomedical signals. He has been collaborating with researchers from NIMHANS, Bangalore, in applying signal processing techniques to various problems in the area of neuroscience. He worked in the Biomedical Engineering Research Centre at Nanyang Technological University in Singapore, as a visiting faculty and worked in the application of digital signal processing to cardiovascular signals. He has published a large number of papers in this area in leading international journals.